Turkish Journal of Electrical Engineering & Computer Sciences

http://journals.tubitak.gov.tr/elektrik/

Research Article

Turk J Elec Eng & Comp Sci
(2018) 26: 1093 – 1102

doi:10.3906/elk-1707-95

Electrostatic discharge currents and their derivatives' approximation by piecewise power-exponential functions

Vesna JAVOR[1,*], **Karl LUNDENGÅRD**[2], **Milica RANČIĆ**[2], **Sergei SILVESTROV**[2]
[1]Department of Power Engineering, Faculty of Electronic Engineering, University of Niš, Niš, Serbia
[2]Division of Applied Mathematics, UKK, Mälardalen University, Västerås, Sweden

Received: 08.07.2017 • **Accepted/Published Online:** 14.11.2017 • **Final Version:** 30.03.2018

Abstract: An analytically extended function based on power-exponential functions is used in this paper for approximation of electrostatic discharge (ESD) currents and their derivatives. The Marquardt least-squares method (MLSM) is applied for obtaining nonlinear function parameters. IEC 61000-4-2 Standard ESD current is approximated, as well as some measured ESD currents' wave shapes. Power-exponential terms are extended at the local maxima and minima of the represented wave shape, so that this approximation is done from peak to peak. ESD current derivative is approximated using the same procedure in order to obtain the continuous second order derivative of the current, as all piecewise functions are of differentiability class C^1. Currents and their derivatives are often measured in ESD experiments so that their analytical representation is needed for simulation of ESD phenomena, better definition of standard requirements, and computation of the transient fields and induced effects.

Key words: Electrostatic discharge currents, N-peaked analytically extended function, Marquardt least-squares method, power-exponential function

1. Introduction

Electrostatic discharges are important phenomena that are intentionally produced in applications or unintentionally induced in working places, in technological processes, or in everyday life. On a large scale, as lightning discharges, they cause damage and failures, affect power systems, and may result in fatal consequences. Mathematical expressions used for representation of electrostatic discharge (ESD) currents and lightning discharge currents are often based on exponential functions. Although typical lightning currents are of the order of kA, whereas other ESD currents are usually of the order of A, these currents' wave shapes are approximated by similar analytical expressions.

Double-exponential function [1,2] is widely used in the literature for pulse wave shape approximations, although is first derivative at the onset time ($t = 0$) is not zero, as in realistic cases. Heidler's function [3] may approximate some typical lightning currents from IEC 62305 Standard [4], as well as IEC 61000-4-2 Standard ESD current [5]. It is differentiable and its first derivative is of zero value at $t = 0$, but it cannot be integrated analytically [6]. Sums of two or more of these functions [7,8], or combinations with other functions [9], are used in the literature in order to better represent lightning current wave shapes. A pulse function [10] may be integrated, but it has peak-correction factors, as well as Heidler's function. These factors have to be recalculated from other nonlinear function parameters for the represented wave shape.

*Correspondence: vesna.javor@elfak.ni.ac.rs

If the N-peaked analytically extended function (NP-AEF) is used for approximation of some current wave shape, the exact peak values at corresponding time moments are chosen prior to the procedure for obtaining its parameters. Its power-exponential terms are extended at N peaks, i.e. at the chosen local maxima or minima of the represented wave shape. There is no need for peak correction factors and there are analytically obtained derivative, integral, and Fourier transform [11]. However, the second order derivative of any piecewise function is not continuous. If ESD current's first derivative is approximated by another NP-AEF, then the NP-AEF's first derivative may be obtained as continuous. As it represents the second order derivative of the current, the problem is circumvented in this way. The same procedure may be further applied to higher order derivatives and thus generalized. In cases of measured currents, which usually have more than a few peaks, NP-AEF has fewer parameters to be determined if compared to other functions from the literature for the same accuracy of approximation [12,13]. The procedure for obtaining NP-AEF's parameters is based on the Marquardt least-squares method (MLSM) [14], which is used in [15] and [16].

NP-AEF and its properties are described in Section 2. Parameters of the three 1P-AEFs, 2P-AEFs, and 3P-AEFs are determined so to approximate IEC 61000-4-2 Standard ESD current. Measured ESD currents are also represented by NP-AEFs and some examples are given in Section 3. ESD current derivatives' approximations are presented in Section 4. The examples show that this procedure for obtaining values of the chosen number of parameters, depending on the accuracy of approximation, may be generalized and applied to various measured ESD currents and their derivatives. These approximations are needed for defining the performance of ESD simulators used in immunity testing according to IEC 61000-4-2 for the contact discharge, for simulations of ESD phenomena, for evaluation of susceptibility of electronic devices against contact discharge, and for estimation of the transient field.

2. Approximation of the IEC 61000-4-2 Standard current by NP-AEF

The generalized NP-AEF, for $N \geq 2$ peaks, is

$$i(t) = \begin{cases} I_{m\,1} \sum\limits_{i=1}^{k_1} b_{1i} \left[\frac{t}{t_{m\,1}} \exp\left(\frac{t_{m\,1}-t}{t_{m\,1}} \right) \right]^{a_{1\,i}}, & 0 \leq t \leq t_{m1} \\ \sum\limits_{j=1}^{n-1} I_{m\,j} + I_{mn} \sum\limits_{i=1}^{k_n} b_{ni} \left[\frac{t-t_{m\,n-1}}{t_{m\,n}-t_{m\,n-1}} \exp\left(\frac{t_{m\,n}-t}{t_{m\,n}-t_{m\,n-1}} \right) \right]^{a_{n\,i}}, & t_{mn-1} \leq t \leq t_{mn}, \\ & n = 2\,, ...,\ N \\ \left(\sum\limits_{j=1}^{N} I_{m\,j} \right) \sum\limits_{i=1}^{k_{N+1}} b_{N+1\,i} \left[\frac{t}{t_{m\,N}} \exp\left(\frac{t_{m\,N}-t}{t_{m\,N}} \right) \right]^{a_{N+1\,i}}, & t_{mN} \leq t < \infty \end{cases} \tag{1}$$

for parameters a_{1i}, a_{ni}, a_{N+1i}, b_{1i}, b_{ni}, and b_{N+1i}. Parameters b satisfy N+1 relations

$$\sum_{i=1}^{k_i} b_{ni} = 1, \quad \text{for } n = 1, ..., N+1, \tag{2}$$

which results in decreasing of the number of unknowns.

The current value of the n-th peak is $\sum\limits_{j=1}^{n} I_{mj}$ at t_{mn}, for n =1,..., N. Index m refers to the local maximum or minimum, i.e. to the chosen peak. I_{mj} is the difference between the j-th and (j-1)-th current peak value. The function starts from the zero value. The n-th interval (for n =1,..., N) is the interval between the n-th and the (n-1)-th peak. The number of terms is k_n in the n-th interval and k_{N+1} in the last (N+1)-th

interval after the N-th peak. Better accuracy of the wave shape approximation is obtained for a greater number of terms, but more unknown parameters have to be determined in that case. As any term has one a_{ni} and one b_{ni} parameter, the number of unknown parameters is $2\,k_n$ for the n-th interval, so that in the case of the NP-AEF and due to (2) the total number of unknowns is

$$K = 2\sum_{n=1}^{N+1} k_n - N - 1. \tag{3}$$

The simplest 1P-AEF [17] has two parameters a_1 and a_2, and a single peak I_m at t_m, whereas $b_1 = b_2 = 1$. It is given by

$$i\,(t) = \begin{cases} I_m \left[\frac{t}{t_m}\,\exp\,\left(\frac{t_m - t}{t_m}\right)\right]^{a_1}, & 0 \le t \le t_m \\ I_m \left[\frac{t}{t_m}\,\exp\,\left(\frac{t_m - t}{t_m}\right)\right]^{a_2}, & t_m \le t < \infty \end{cases} \tag{4}$$

This function is denoted by 1P-AEF(1,1), as there is one term in the first interval from zero value to the peak ($t < t_m$), and one term in the second interval after the peak ($t > t_m$). It may approximate lightning currents from the IEC 62305 Standard [4].

ESD simulator verification current for testing in the contact mode is given in the IEC 61000-4-2 Standard [5] and presented in Figure 1. This waveform has a few peaks that have to be taken into account. There are a few functions in the literature [18–24] used for approximation of this Standard ESD current, but NP-AEF results in a better approximation of the current wave shape.

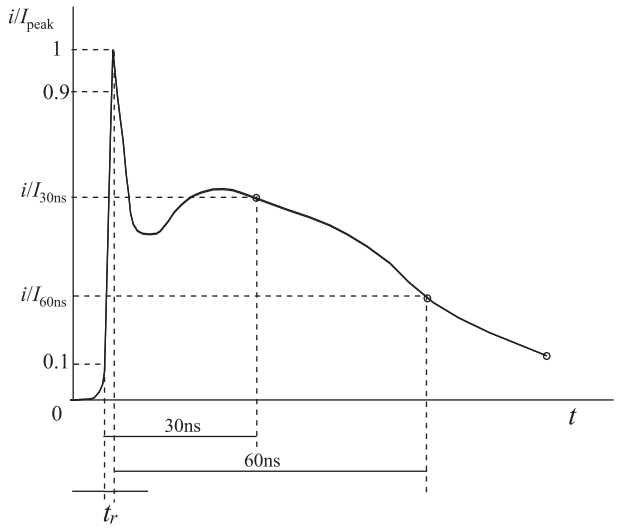

Figure 1. The IEC 61000-4-2 Standard ESD current waveform [5].

Application of the contact discharges using ESD simulators is usually done for testing according to the IEC 61000-4-2. The contact discharge is a preferred test method, but the air discharge is used where the contact discharge cannot be applied. For the air discharges, test voltages range from 2 kV to 15 kV, and for the contact discharges from 2 kV to 8 kV, as given in the Table. It has to be noted that ESD test generator current performance depends significantly on various conditions, such as charging voltages, humidity, temperature, approach speeds, types of electrodes, and relative arc length. The tolerances of the characteristic ESD current parameters are given in the Table.

Table. ESD contact mode simulator current specification from IEC 61000-4-2.

ESD voltage [kV]	I_{peak}[A]	Rise time t_r [ns]	I_{30ns}[A]	I_{60ns}[A]
2	7.5 ± 15%	0.8 ± 25%	4 ± 30%	2 ± 30%
4	15 ± 15%	0.8 ± 25%	8 ± 30%	4 ± 30%
6	22.5 ± 15%	0.8 ± 25%	12 ± 30%	6 ± 30%
8	30 ± 15%	0.8 ± 25%	16 ± 30%	8 ± 30%

Current values depend on discharge voltage V, so that [5] defines $I_{peak}/V = 3.75$ A/kV, $I_{30ns}/V = 2$ A/kV at $t = 30$ ns, and $I_{60ns}/V = 1$ A/kV at $t = 60$ ns, if time is calculated from the moment when current has 10% of its I_{peak} value (Figure 1). Rise time t_r is the difference between the time moments corresponding to 10% I_{peak} and 90% I_{peak}. For the discharge voltage $V = 4$ kV and the current peak $I_{peak} = 15$ A, approximations of the Standard ESD current by various functions are presented in Figures 2 and 3.

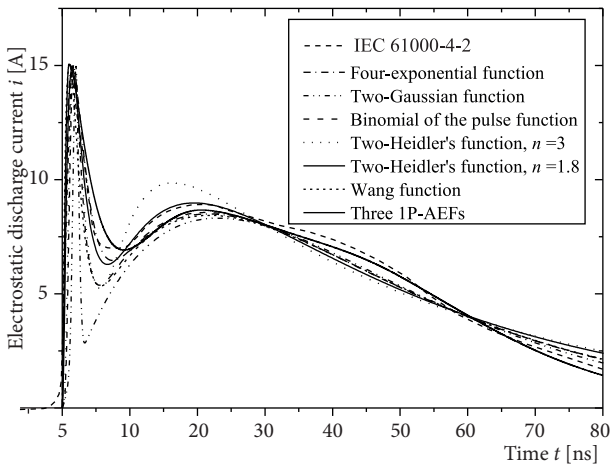

Figure 2. Functions for approximation of the IEC 61000-4-2 current for 4 kV.

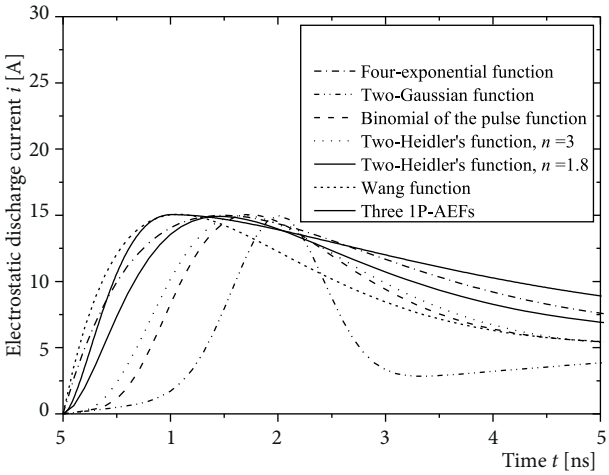

Figure 3. Functions for approximation of the IEC 61000-4-2 current in the first 5 ns.

Four-exponential function [18] is

$$i(t) = i_1\,[\exp(-t/\tau_1) - \exp(-t/\tau_2)] + i_2\,[\exp(-t/\tau_3) - \exp(-t/\tau_4)]\,, \tag{5}$$

for $i_1 = 498$ A, $i_2 = 148.5$ A, $\tau_1 = 1.4$ ns, $\tau_2 = 1.3$ ns, $\tau_3 = 23.37$ ns, and $\tau_4 = 20$ ns, denoted by the dash-dot lines in Figures 2 and 3.

The two-Gaussian function [19] is

$$i(t) = A\,\exp\left[-(t-t_1)^2/\sigma_1^2\right] + B\;t\,\exp\left[-(t-t_2)^2/\sigma_2^2\right]\,, \tag{6}$$

for $A = 13.25$ A, $B = 391$ A/ns, $t_1 = 2$ ns, $t_2 =$ -300 ns, $\sigma_1 = 0.6$ ns, and $\sigma_2 = 122.2$ ns, denoted by the dash–dot–dot lines in Figures 2 and 3.

The binomial expression [20-21] of the pulse function [10] is

$$i(t) = I_0\,[1 - \exp(-t/\tau_1)]^{\,p}\exp(-t/\tau_2) + I_1\,[1 - \exp(-t/\tau_3)]^{\,q}\exp(-t/\tau_4), \tag{7}$$

for $I_0 = 106.5$ A, $I_1 = 60.5$ A, $\tau_1 = 0.62$ ns, $\tau_2 = 1.1$ ns, $\tau_3 = 55$ ns, $\tau_4 = 26$ ns, p = 8, q = 1, and is denoted by the long-dash lines in Figures 2 and 3.

The two-Heidler's function [3] proposed in [22] is

$$i\left(t\right)=\left(\frac{i_1}{\eta_1}\right)\frac{\left(t/\tau_1\right)^n}{1+\left(t/\tau_1\right)^n}\exp\left(-\frac{t}{\tau_2}\right)+\left(\frac{i_2}{\eta_2}\right)\frac{\left(t/\tau_3\right)^n}{1+\left(t/\tau_3\right)^n}\exp\left(-\frac{t}{\tau_4}\right), \tag{8}$$

for $n=3$, $i_1=17.5$ A, $i_2=10.1$ A, $\tau_1=1.3$ ns, $\tau_2=1.7$ ns, $\tau_3=8.7$ ns, and $\tau_4=42$ ns, denoted by the dotted lines in Figures 2 and 3. For the Standard IEC 61000-4-2 [5] current and for. $n=1.8$ the parameters are calculated in [23] as the following: $i_1=16.6$ A, $i_2=9.3$ A, $\tau_1=1.1$ ns, $\tau_2=2.0$ ns, $\tau_3=12$ ns, $\tau_4=37$. It is denoted by the solid lines in Figures 2 and 3. Heidler's function has peak correction factor $\eta_1=\exp\left[-\left(\tau_1/\tau_2\right)\sqrt[n]{n\tau_2/\tau_1}\right]$ for the first term and $\eta_2=\exp\left[-\left(\tau_3/\tau_4\right)\sqrt[n]{n\tau_4/\tau_3}\right]$ for the second term in (8).

The Wang function [24] is

$$i(t)=A\,t\,\exp\left[-Ct\right]+B\,t\,\exp\left[-Dt\right], \tag{9}$$

for $A=38.1679$ A/ns, $B=1.0526$ A/ns, $C=1$/ns, $D=0.0459$/ns, denoted by the short-dash lines in Figures 2 and 3. Rising parts of the functions given (5)-(9) are presented in Figure 3 in the first 5 ns.

Approximations of the IEC 61000-4-2 current by NP-AEFs presented in this paper are: a) Sum of the three 1P-AEFs(1,1), b) 2P-AEF(1,2,2); c) 2P-AEF(1,3,4); d) 3P-AEF(2,2,2,4); and e) 3P-AEF(1,2,2,4). The numbers in brackets denote the numbers $k_1, k_2, \ldots, k_n$ of the applied terms in the corresponding time intervals between the peaks of AEF given by (1).

a) Sum of the three 1P-AEFs, for the discharge voltage 4 kV, has the initial peak current $I_{peak}=15$ A, $I_{30ns}=8$ A, and $I_{60ns}=4$ A, as in [5], as well as other functions [18–23] for the Standard IEC 61000-4-2 current approximation and it is denoted by the thick solid lines in Figures 2 and 3.

b) Sum of the three 1P-AEFs is a function given by

c) $$i\left(t\right)=\sum_{k=1}^{3}i_k(t)=\begin{cases} I_{m\,k}\left[\frac{t}{t_{m\,k}}\exp\left(1-\frac{t}{t_{m\,k}}\right)\right]^{a_{k1}}, & 0\le t<t_{m\,k} \\ I_{m\,k}\left[\frac{t}{t_{m\,k}}\exp\left(1-\frac{t}{t_{m\,k}}\right)\right]^{a_{k2}}, & t_{m\,k}\le t<\infty \end{cases} \tag{10}$$

d) for $I_{\,m1}=15$ A, $I_{\,m2}=8.55$ A, $I_{\,m3}=1.8$ A, at $t_{\,m1}=1$ ns, $t_{\,m2}=21$ ns, $t_{\,m3}=50$ ns. The currents values $I_{\,m1}$, $I_{\,m2}$, and $I_{\,m3}$ denote the single peaks of the three different functions 1P-AEF as given by (4). The ESD current function $i(t)$ is also presented in Figure 4 with its components $i_{\,1}$, $i_{\,2}$, and $i_{\,3}$. This decomposition may be useful for simulation of ESD by electric circuits. Each 1P-AEF(1,1) has 2 parameters to be determined, so that the total number of a parameters is 6, and they are determined as $a_{\,11}=2.0$, $a_{\,12}=0.3$, $a_{\,21}=2.5$, $a_{\,22}=1.5$, $a_{\,31}=15$, $a_{\,32}=10$.

e) All of the functions from the literature [18–24] start rising faster than the standard current wave shape given in Figure 1, and do not approximate the first 6 ns of the standard wave shape, as may be noted in Figure 2.

f) Time of the maximum $t_{\,m}$ is between 1 ns and 2 ns, which is less than in Figure 1, although their rise time $t_{\,r}$ is in the range defined by [5]. None of them reproduce a hump in the decaying part of current wave shape. However, NP-AEF may reproduce the Standard wave shape better, if more peaks and terms are chosen, and also a very slow start up to 10% of its $I_{\,peak}$ value, whereas rise time $t_{\,r}$ as defined in [5].

g) 2P-AEF(1,2,2) with 1 term in the first interval from zero up to the first maximum and 2 terms in the next two intervals, is the simplest AEF that well approximates the Standard ESD current [5], as presented in Figure 5. It is denoted by the dashed line in Figure 5. This function, for N = 2 in (1), numbers of terms $k_1 = 1$, $k_2 = 2$, and $k_3 = 2$, has $K = 7$ unknown parameters, peaks $I_{m1} = 15$ A at $t_{m1} = 6.89$ ns, and $I_{m1} + I_{m2} = 9.0921$ A at $t_{m2} = 25.54$ ns, as the difference is $I_{m2} = -5.9079$ A between the lower second and the higher first peak. Its parameters are determined as the following: $a_{11} = 183.25$, ($b_{11} = 1$), $a_{21} = 1.452$, $a_{22} = 1.656$, $b_{21} = 19.481$, ($b_{22} = 1 - b_{21} = -18.481$), $a_{31} = 1.785$, $a_{32} = 4.60$, $b_{31} = 1.287$, ($b_{32} = 1 - b_{31} = -0.287$). However, it does not represent the hump as well as 2P-AEFs with more terms. It has the rise time $t_r = 0.8$ ns.

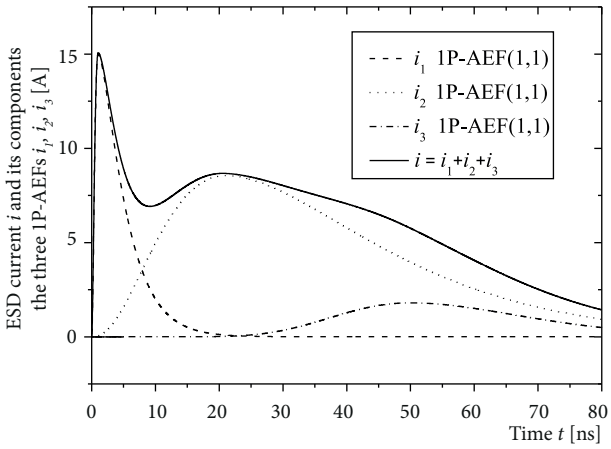

Figure 4. ESD current i as a sum of the three 1P-AEFs: i_1, i_2, and i_3.

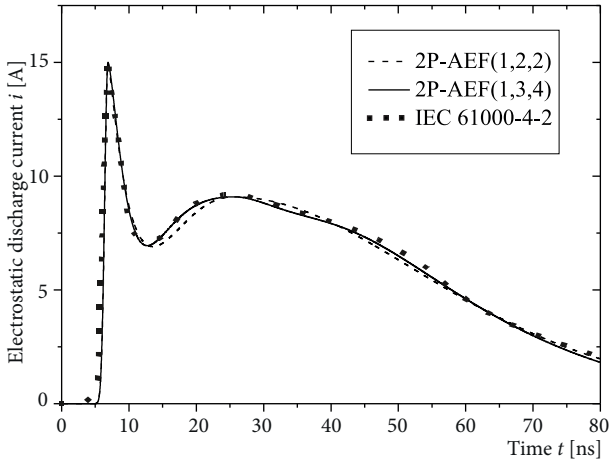

Figure 5. 2P-AEF(1,2,2), 2P-AEF(1,3,4), and the IEC 61000-4-2 Standard current.

h) 2P-AEF(1,3,4) has the same two peaks as 2P-AEF(1,2,2), but more terms: $k_1 = 1$, $k_2 = 3$, and $k_3 = 4$, so that K =13 unknown parameters are determined by using MLSM as the following: $a_{11} = 183.25$, ($b_{11} = 1$), $a_{21} = 1.4665$, $a_{22} = 3.0736$, $a_{23} = 3.2741$, $b_{21} = 7.202$, $b_{22} = -43.423$, ($b_{23} = 1 - b_{21} - b_{22} = 37.221$), $a_{31} = 0.0416$, $a_{32} = 1.7056$, $a_{33} = 9.2477$, $a_{34} = 21.4184$, $b_{31} = -0.037$, $b_{32} = 1.275$, $b_{33} = -0.453$, ($b_{34} = 1 - b_{31} - b_{32} - b_{33} = 0.215$). It is denoted by the solid line in Figure 5. Its derivative is given in Figure 6. It has the rise time $t_r = 0.8$ ns.

i) 3P-AEF(2,2,2,4) has a very slow start of the function. Although it corresponds well to the graphical representation in [5], its rise time is $t_r = 1.5$ ns, which is outside the acceptable range $t_r = 0.8$ ns $\pm 25\%$. It is denoted by the dotted line in Figure 7.

j) 3P-AEF(1,2,2,4) has the rise time $t_r = 0.8$ ns, follows well the Standard current wave shape [5], and is denoted by the solid line in Figure 7. This function, for N = 3 peaks in (1), for the numbers of terms $k_1 = 1$, $k_2 = 2$, $k_3 = 2$, and $k_4 = 4$, has $K = 14$ unknown parameters. Its current peaks are $I_{m1} = 15$ A, $I_{m1} + I_{m2} = 7.1484$ A, and $I_{m1} + I_{m2} + I_{m3} = 9.0921$ A at $t_{m1} = 6.89$ ns, $t_{m2} = 12.85$ ns, and $t_{m3} = 25.54$ ns. NP-AEF's parameters are calculated by using MLSM so that: $a_{11} = 183.25$, ($b_{11} = 1$), $a_{21} = 1.510$, $a_{22} = 29.037$, $b_{21} = 1.094$, ($b_{22} = 1 - b_{21} = -0.094$), $a_{31} = 3.390$, $a_{32} = 3.762$, $b_{31} = 6.28$, ($b_{32} = 1 - b31 = -5.28$), $a_{41} = 0.041616$, $a_{42} = 1.705636$, $a_{43} = 9.2477$, $a_{44} = 21.4184$, $b_{41} =$

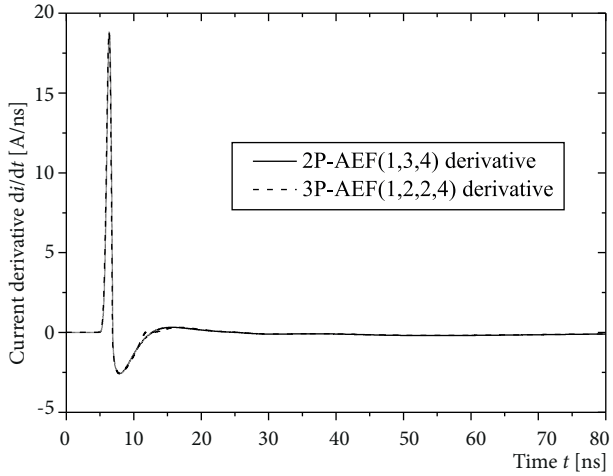

Figure 6. First derivatives of the currents 2P-AEF(1,3,4) and 3P-AEF(1,2,2,4).

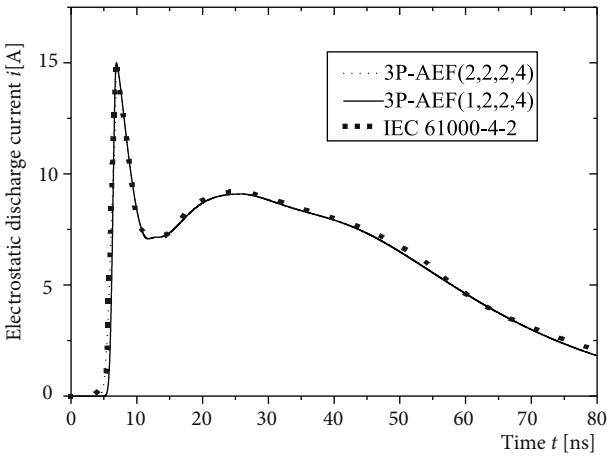

Figure 7. 3P-AEF(2,2,2,4), 3P-AEF(1,2,2,4) and the IEC Standard 61000-4-2 current.

–0.037, b_{42} = 1.275, b_{43} = -0.453, (b_{44} = 1 – b_{41} – b_{42} – b_{43} = 0.215). Its derivative is also presented in Figure 6. It may be noted that this approximation of the IEC 61000-4-2 Standard current is very similar to approximation with 2P-AEF(1,3,4), as the total number of function parameters is almost the same. If more peaks are used, then fewer terms are needed per interval for the same accuracy of approximation.

3. Approximation of the measured ESD currents by NP-AEF

For experimentally measured ESD current of the contact human-to-metal discharge, for 2 kV voltage [25], MLSM is applied to obtain an adequate approximation [17] by NP-AEF as given by (1). 3P-AEF(1,2,2,4), which approximates this ESD current [25], is denoted by the thick-dash–dot line in Figure 8. This function, for N = 3 and numbers of terms k_1 = 1, k_2 = 2, k_3 = 2, and k_4 = 4, has its peaks I_{m1} = 7.37 A, $I_{m1} + I_{m2}$ = 5.02 A, $I_{m1} + I_{m2} + I_{m3}$ = 3.82 A at the time moments t_{m1} = 1.23 ns, t_{m2} = 6.39 ns, and t_{m3} = 15.5 ns, so that K = 14 parameters have to be determined.

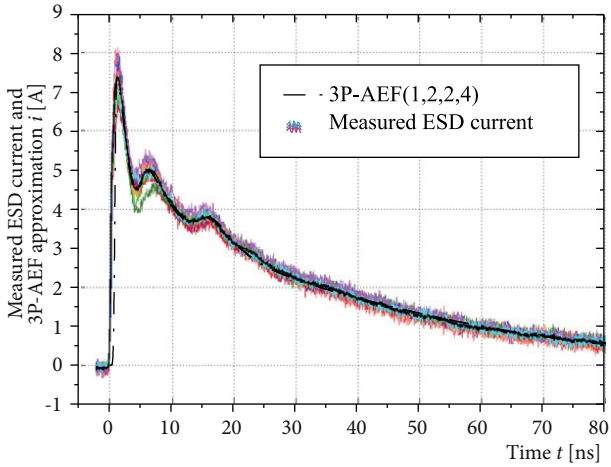

Figure 8. Measured ESD current [25] and its 3P-AEF(1,2,2,4) approximation.

Using the MLSM, parameter values are obtained as the following: $a_{11} = 17.701$, ($b_{11} = 1$), $a_{21} = 1.765$, $a_{22} = 9.908$, $b_{21} = 1.094$, ($b_{22} = 1 - b_{21} = -0.094$), $a_{31} = 1.496$, $a_{32} = 53.958$, $b_{31} = 6.28$, ($b_{32} = 1 - b_{31} = -5.28$), $a_{41} = 1.3322$, $a_{42} = 0.6597$, $a_{43} = 5.784$, $a_{44} = 22.6481$, $b_{41} = -0.037$, $b_{42} = 1.275$, $b_{43} = -0.453$, ($b_{44} = 1 - b_{41} - b_{42} - b_{43} = 0.215$). The derivative of this function is presented in Figure 9.

4. Approximation of the measured ESD current derivative by NP-AEF

Current derivatives are often measured in ESD experiments. 17P-AEF is used for approximation of the measured ESD current derivative [26], as presented in Figure 10, with 17 peaks at the corresponding time moments, denoted by crosses. For one term in each interval, there are 18 unknown parameters. For similar accuracy of approximation, e.g., 6P-AEF with two terms in each interval may be used, or 3P-AEF with four terms in each interval.

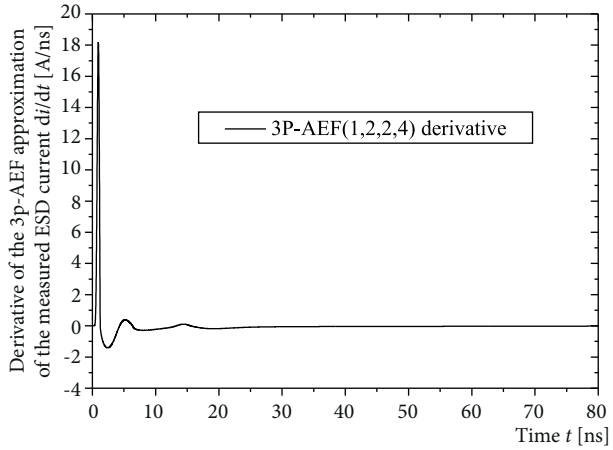

Figure 9. Derivative of the measured ESD current approximated by 3P-AEF(1,2,2,4).

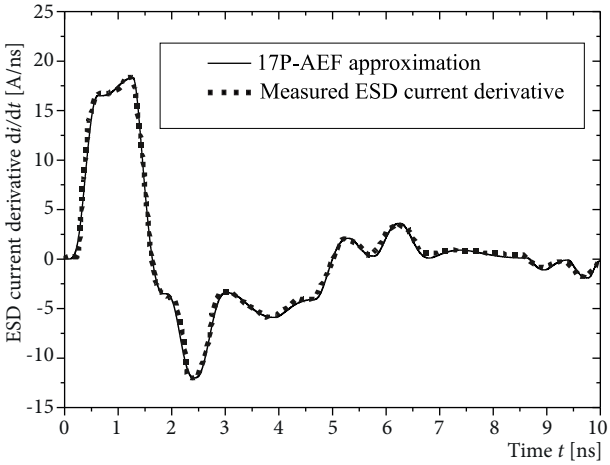

Figure 10. Measured ESD current derivative for the simulator A [26] and its 17P-AEF approximation.

If 17P-AEF, which approximates the current derivative, is integrated, then the current denoted by the solid line in Figure 11 is obtained. The measured current is also presented in Figure 11 for this case. It is also important to note that the 17P-AEF representation of the first derivative may be differentiated further.

It may be also done vice versa, so if the measured current given in Figure 11 is approximated, e.g. by 3P-AEF, its first derivative may be obtained from it.

5. Conclusion

Calibration and verification of measurement equipment request standard current waveform defined as a mathematical equation, as well as clearly defined measurement uncertainty for different environmental conditions and testing parameters [27]. In order to protect electronic components and electric systems from ESD damage, it is very important to estimate the total delivered energies and the peaks of ESD currents waveforms. Specific energy may be calculated as the integral of the square of the current function. The current derivative represents the current's rate of rise and decay, so that approximation of its wave shape is also important for the ESD testing. NP-AEFs are used in this paper for approximation of the IEC 61000-4-2 Standard current, for measured ESD currents and their derivatives. These functions apply linear combinations of power-exponential terms that provide good accuracy of obtained approximations for various wave shapes. Local maxima and/or minima at

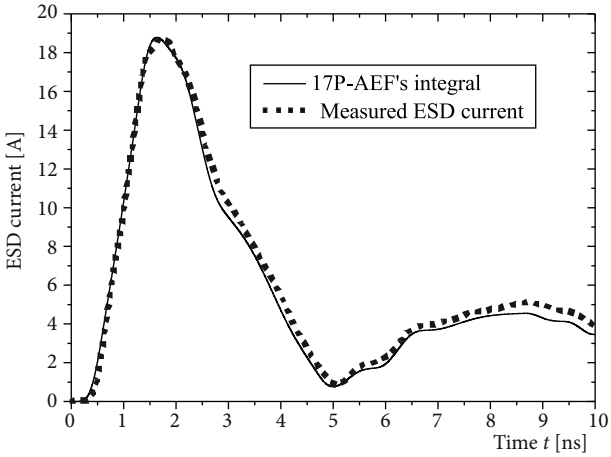

Figure 11. Measured ESD current for the simulator A [26] and integral of the 17P-AEF approximation from Figure 10.

corresponding time moments are chosen as the peaks of NP-AEFs, so that approximation is done "from peak to peak". If more peaks are used, then fewer terms are needed per interval between the peaks for the same accuracy of approximation. The MLSM is applied for obtaining nonlinear function parameters. NP-AEFs may be used for the synthesis of circuits capable of producing ESD current wave shapes, in simulations of ESD events, and in modelling and precompliance testing of immunity, emissions, and susceptibility of EUTs. However, the nature of ESD phenomena is very complex, so that the insight into physical mechanisms requires further research.

Acknowledgments

The authors are grateful to Dr Pavlos Katsivelis from the High Voltage Laboratory, School of Electrical and Computer Eng., National Technical University of Athens, Greece, for the measured ESD current data. The research presented in this paper is supported in part by the Ministry of Education, Science and Technological Development of the Republic of Serbia (project HUMANISM III 44004).

References

[1] Bruce CER, Golde RH. The lightning discharge. J Inst Electr Eng 1941; 88: 487-520.

[2] Golde RH. Lightning currents and related parameters. In: Lightning vol 1, Physics of Lightning, London, UK: Academic Press, 1977, pp. 309-350.

[3] Heidler F. Travelling current source model for LEMP calculation. In: 6th Int. Zurich Symp. EMC Proc. 1985; pp. 157-162.

[4] IEC 62305-1 standard, Protection against lightning – Part 1: General principles, Ed.2.0, 2010-12.

[5] IEC 61000-4-2 standard, EMC – Part 4-2: Testing and Measurement Techniques – Electrostatic Discharge Immunity Test, Ed.2.0, 2008-2012.

[6] Heidler F, Cvetic J. A class of analytical functions to study the lightning effects associated with the current front. Eur T Electr Power 2002; 12: 141-150.

[7] Diendorfer G, Uman MA. An improved return stroke model with specified channel-base current. J Geophys Res 1990; 95: 13621-13644.

[8] Nucci CA, Diendorfer G, Uman MA, Rachidi F, Ianoz M, Mazzetti C. Lightning return stroke current models with specified channel-base current: a review and comparison. J Geophys Res 1990; 95(D12): 20395-20408.

[9] Rakov VA, Uman MA. Review and evaluation of lightning return stroke models including some aspects of their application. IEEE T Electromagn C 1998; 40: 403-426.

[10] Feizhou Z, Shange L. A new function to represent the lightning return-stroke currents. IEEE T Electromagn C 2002; 44: 595-597.

[11] Javor V. Multi-peaked functions for representation of lightning channel-base currents. In: ICLP 2012 31st International Conference on Lightning Protection; Vienna, Austria. doi:10.1109/ICLP.2012.6344384.

[12] De Conti A, Visacro S. Analytical representation of single- and double-peaked lightning current waveforms. IEEE T Electromagn C 2007; 49: 448-451.

[13] Javor V. Approximation of a double-peaked lightning channel-base current. COMPEL 2012; 31: 1007-1017.

[14] Marquardt DM. An algorithm for least-squares estimation of non-linear parameters. J Soc Ind Appl Math 1963; 11: 431-441.

[15] Lovrić D, Vujević S, Modrić T. On the estimation of Heidler function parameters for reproduction of various standardized and recorded lightning current waveshapes. Int T Electr Energy 2013; 23: 290-300.

[16] Lundengärd K, Rančić M, Javor V, Silvestrov S. Estimation of parameters for the multi-peaked AEF current functions. Springer Methodology and Computing in Applied Probability 2016; doi: 10.1007/s11009-016-9501-z, pp. 1-15.

[17] Javor V. New function for representing IEC 61000-4-2 Standard electrostatic discharge current. Facta Universitatis Series Electronics & Energetics 2014; 27: 509-522.

[18] Keenan RK, Rosi LKA. Some fundamental aspects of ESD testing. In: IEEE Int. Symp. on Electromagn. Compatibility 1991; New Jersey, USA: IEEE. pp. 236-241.

[19] Berghe SV, Zutter D. Study of ESD signal entry through coaxial cable shields. J Electrostat 1998; 44: 135-148.

[20] Songlin S, Zengjun B, Minghong T, Shange L. A new analytical expression of current waveform in Standard 61000-4-2. High Power Laser & Particle Beams 2003; 15: 464-466.

[21] Yuan Z, Li T, He J, Chen S, Zeng R. New mathematical descriptions of ESD current waveform based on the polynomial of pulse function. IEEE T Electromagn C 2006; 48: 589-591.

[22] Wang K, Pommerenke D, Chundru R, Van Doren T, Drewniak JL, Shashindranath A. Numerical modeling of electrostatic discharge generators. IEEE T Electromagn C 2003; 45: 258-270.

[23] Fotis GP, Ganos IF, Stathopulos IA. Determination of discharge current equation parameters of ESD using genetic algorithms. Electron Lett 2006; 42: 797-799.

[24] Wang K, Wang J, Wang X. Four order electrostatic discharge circuit model and its simulation. Telkomnika 2012; 10: 2006-2012.

[25] Katsivelis PS, Gonos IF, Stathopulos IA. Estimation of parameters for the electrostatic discharge current equation with real human discharge events reference using genetic algorithms. Meas Sci Technol 2010; 21 (105703): 1-6.

[26] Pommerenke D, Aidam M. ESD: Waveform calculation, field and current of human and simulator ESD. J Electrostat 1996; 38: 33-51.

[27] Wright N. New ESD standard and influence on test equipment requirements. Turk J Elec Eng & Comp Sci 2009; 17: 337-344.